

Dokumentenname: ATLAS_TD3.2.docx
Version: 1.0
Ausgabedatum: 17.08.2016

Verfasser: NK
Freigabe: JG

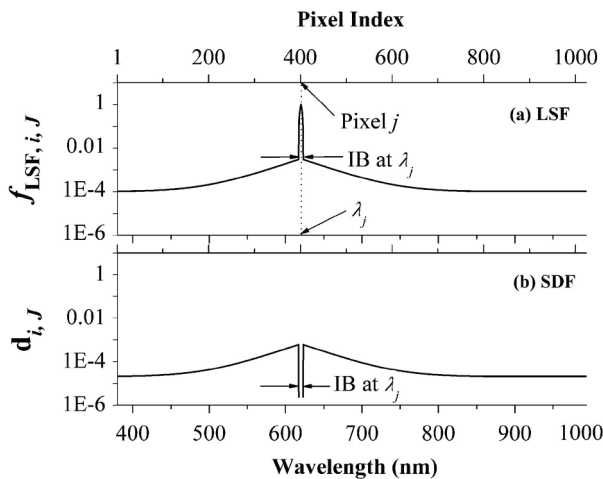
In-range Stray Light Correction methodology for array spectroradiometers

1 Introduction

The measurements of Line Spread Functions (LSF) performed with the ATLAS setup are described in ATLAS_TD2.1 and ATLAS_TD2.2. The LSF measurements are used to establish the in-range stray light correction for array spectroradiometers based on the methodology described in Zong *et al.* (2006).

2 In-range Stray Light Correction

The stray light correction method by Zong *et al.* (2006) is based on measurements of monochromatic spectral lines that cover the whole spectral range of the tested detector. The spectroradiometer's relative response at every pixel i to a fixed monochromatic excitation at wavelength λ_j falling on the pixel $j = J$ is called the spectral Line Spread Function (LSF), denoted $f_{LSF,i,J}$. (Figure 1). The LSF can be separated in a narrow peak region that corresponds to the instrument's bandpass the in-band (IB) response and the remaining broad region that arises from undesired radiation falling on to the detector, spectral stray light, or out-band radiation (OB). The stray light signal distribution function (SDF) denoted $d_{i,J}$, is derived from the corresponding LSF by normalizing the $f_{LSF,i,J}$ to the total IB area and setting values of array elements within the IB area to zero.



$$d_{i,J} = \frac{f_{LSF,i,J}}{\sum_{i \in IB} f_{LSF,i,J}}, i \notin IB$$

$$d_{i,J} = 0, i \in IB$$

$$Y_{meas} = [I + D]Y_{IB}$$

$$Y_{IB} = A^{-1}Y_{meas} = CY_{meas} \text{ eq. 1}$$

Figure 1: Illustration of the LSF of a spectroradiometer with a 1024-pixel array detector. The wavelength of the spectral line source is λ_j , centered on pixel j of the array. (b) Plot of the corresponding SDF derived from the LSF shown in (a). The top x axis is in pixel space, and the bottom x axis is in wavelength space (from Zong *et al.* (2006))

3 LSF for Systems 1 & 2

The LSF of Phaethon (System 1) and PSR_006 (System 2) have been measured with the ATLAS system. For Phaethon, 76 lines have been measured covering the operational range 299-452.2 nm and a dynamic range of 5 orders of magnitude (Figure 2) while for PSR_006, 56 lines were measured covering the range 320-1020.2 nm and a dynamic range of 6 orders of magnitude (Figure 3).

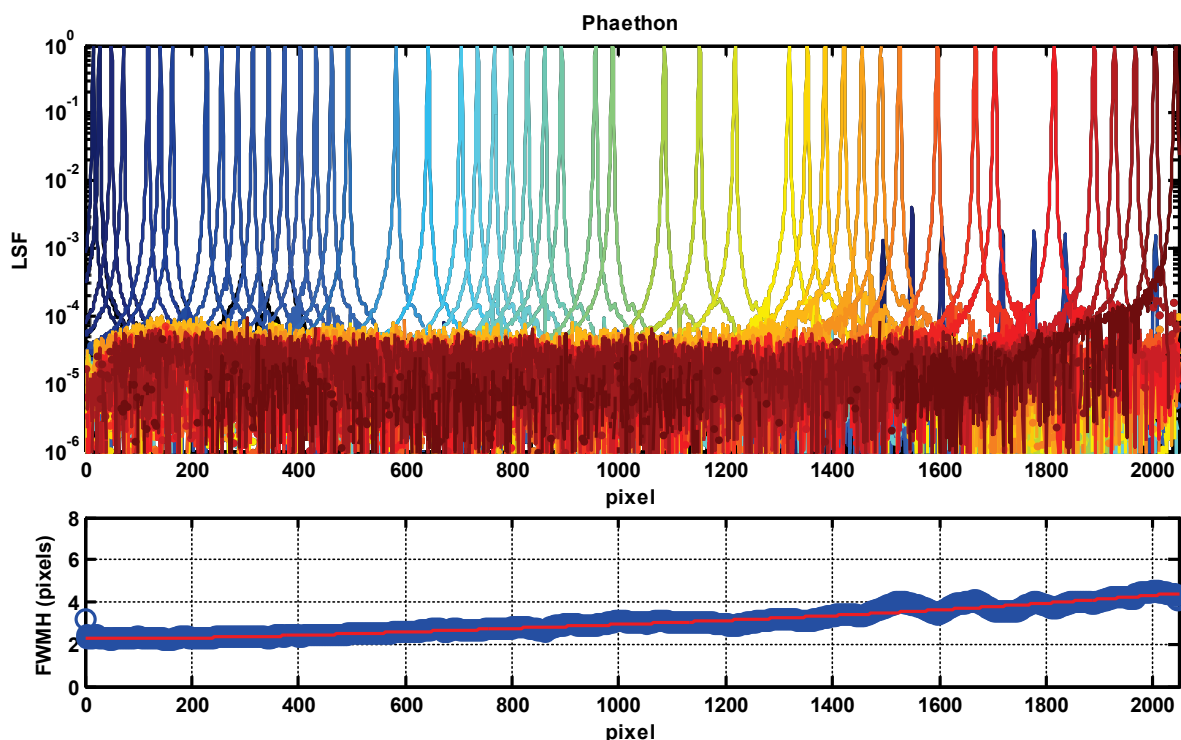


Figure 2 : LSF (top figure) and Full Width at Half Maximum (FWHM), (Bottom figure) of Phaethon measured at 76 wavelengths (299-452.2 nm) with the ATLAS system

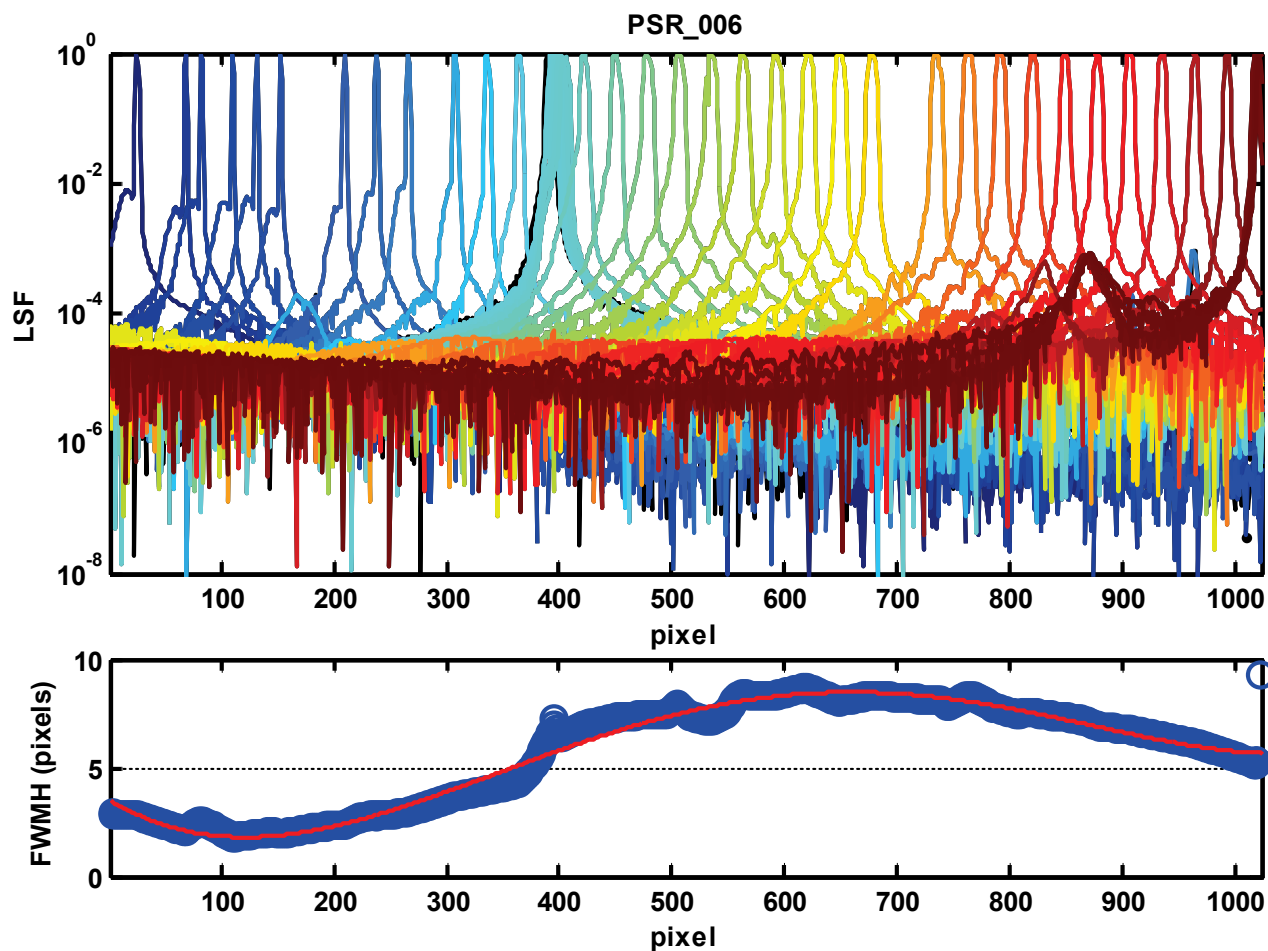


Figure 3 LSF (top figure) and Full Width at Half Maximum (FWHM), (Bottom figure) of PSR measured at 56 wavelengths (320-1020 nm) with the ATLAS system

4 Slit Function Shape

In order to determine the shape of the In-Band region of each spectroradiometer system with high resolution and because of the discrete number of pixels within the slit function, the regions $305 \pm 2 \text{ nm}$ and $381 \pm 4 \text{ nm}$ have been scanned by adjusting the monochromatic radiation from the ATLAS tunable laser with a step of 0.05 nm for Phaethon and PSR_006 respectively. In both cases the normalized spectral shape of the In-Band region, here called slit function (SLF), can be simulated by a double Gaussian fit with an uncertainty of less than 10% over the dark grey areas in Figure 4 and Figure 5.

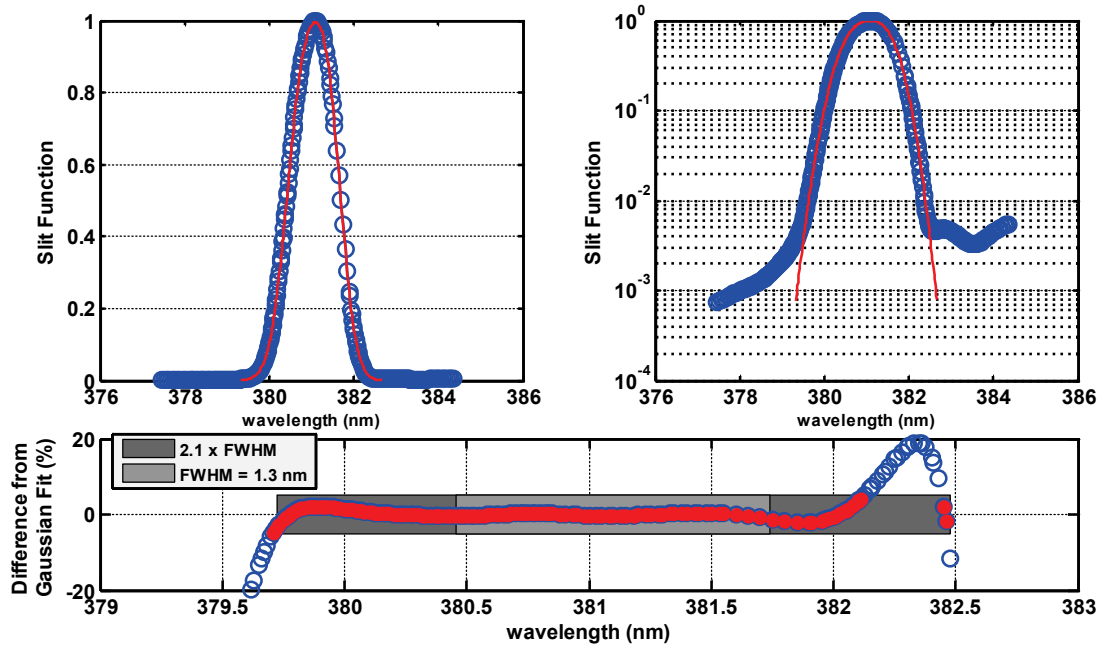


Figure 4: Slit Function (Normalized spectral shape of the In-Band range) for PSR_006, data: blue dots, double Gaussian fit: red line (upper panels) and percentage differences between data and Gaussian fit lower panel. The light gray represents the FWHM while the dark gray area represents the agreement area within 10% which is found to be 2.1 x the FWHM .

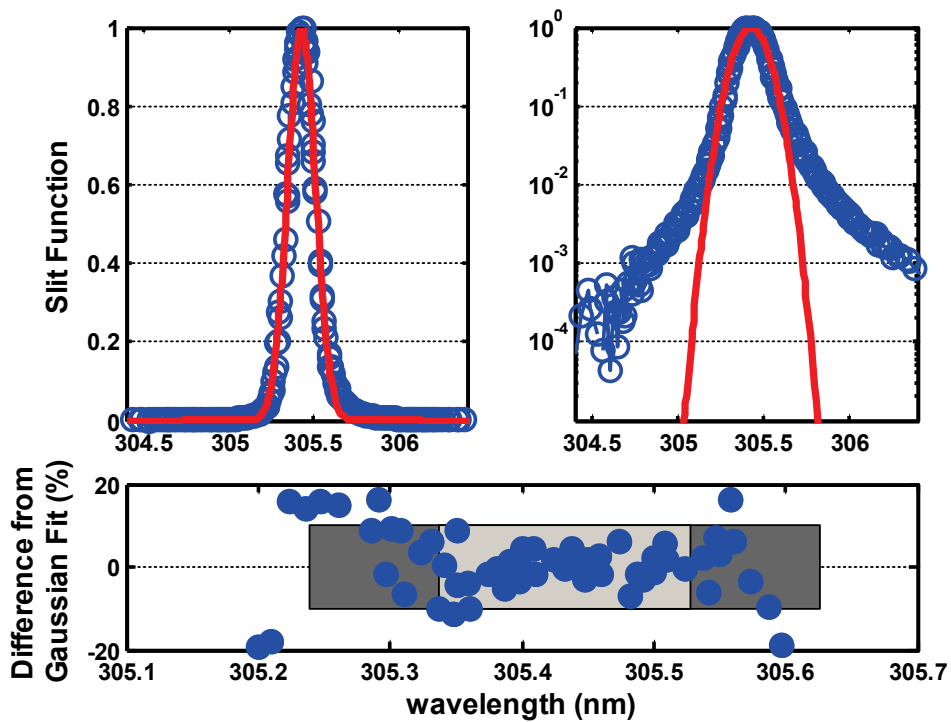


Figure 5: Slit Function (Normalized spectral shape of the In-Band range) for Phaethon, data: blue dots, double Gaussian fit: red line (upper panels) and percentage differences between data and Gaussian fit lower panel. The light gray represents the FWHM while the dark gray area represents the percentage difference within the requested 10%.

5 Determination of the In-Band region

We determined the in-band region as the region which can be simulated by a Gaussian fit with an agreement to the LSFs of better than 10%. For the Gaussian fits we examined the following possibilities:

1. Best fit up to 4th order: for accurate simulation of the SLF and maximum increase of the In-Band region
2. Single Gaussian Fit: for unified simulation over the spectral range, similar to retrieval algorithms (eg QDOAS) that simulate the LSFs with single Gaussian fits with spectrally varying FWHM.

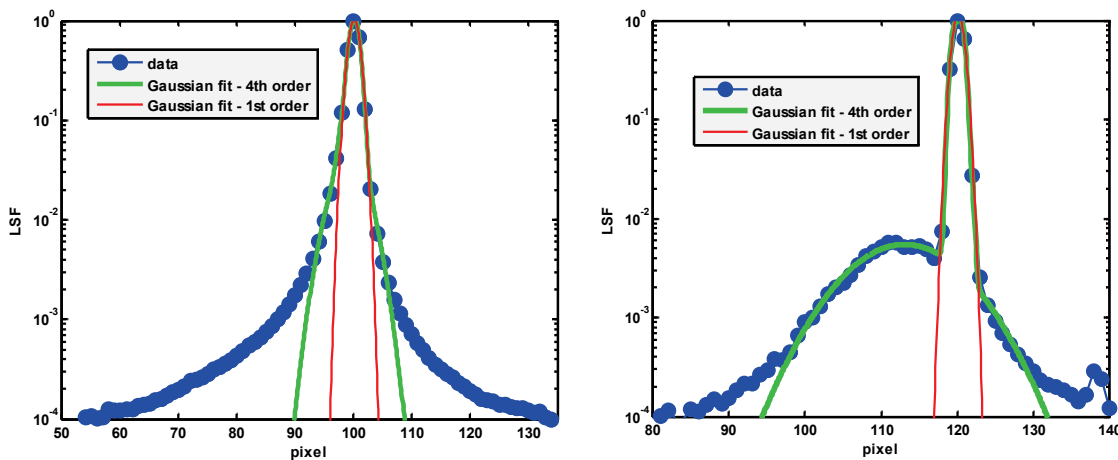


Figure 6: Examples of the Gaussian fits of 1st and 4th order for Phaethon (left) and PSR_006 (right). The IB region considered to be the region where the agreement between the data and fit is better than 10%.

For these two options of the IB range the stray light matrix A (eq 1) has been calculated for both systems. Option 1 returns a quite noisy IB range by switching between different orders of Gaussian fits. To overcome this problem a linear fit over the calculated right and left pixels limits has been applied (denoted as fit), which is considered to be the most stable solution and provides the final Stray Light Correction for each system. Moreover in order to investigate the sensitivity of the correction on the width of the IB region, the width of the stable solution is increased by 1 to 10 pixel in left and right side simultaneously. The width of the IB region for the above mentioned cases for PSR_006 ranges between 6-35 pixels (Figure 7) and for Phaethon between 10-30 pixels (Figure 9). For both systems the single Gaussian fit has the worst performance resulting in IB range 3-10 pixels. The percentage of spectral Stray Light Contribution in Phaethon ranges between 3 -4% (Figure 10) and almost constant of the spectral range. For PSR_006 we observe higher contribution to the UV range, 4%, to decrease to 3% at the NIR range (Figure 8).

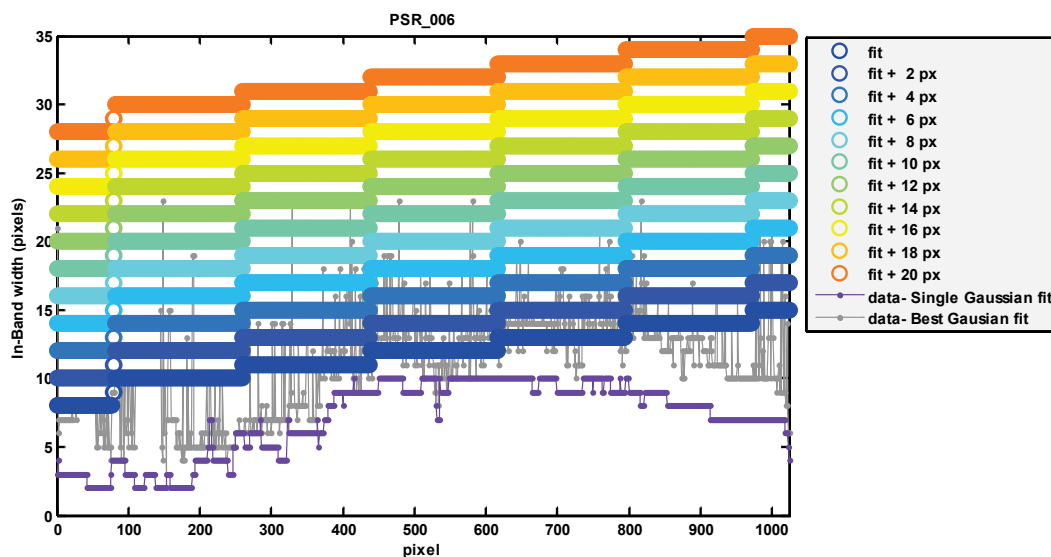


Figure 7: Selection of the In-Band region based on the agreement (better than 10%) between measurement and Gaussian fit. The Violet line represents the single Gaussian fit , the gray line the best Gaussian fit and the dark blue line the linear fit over the gray data.

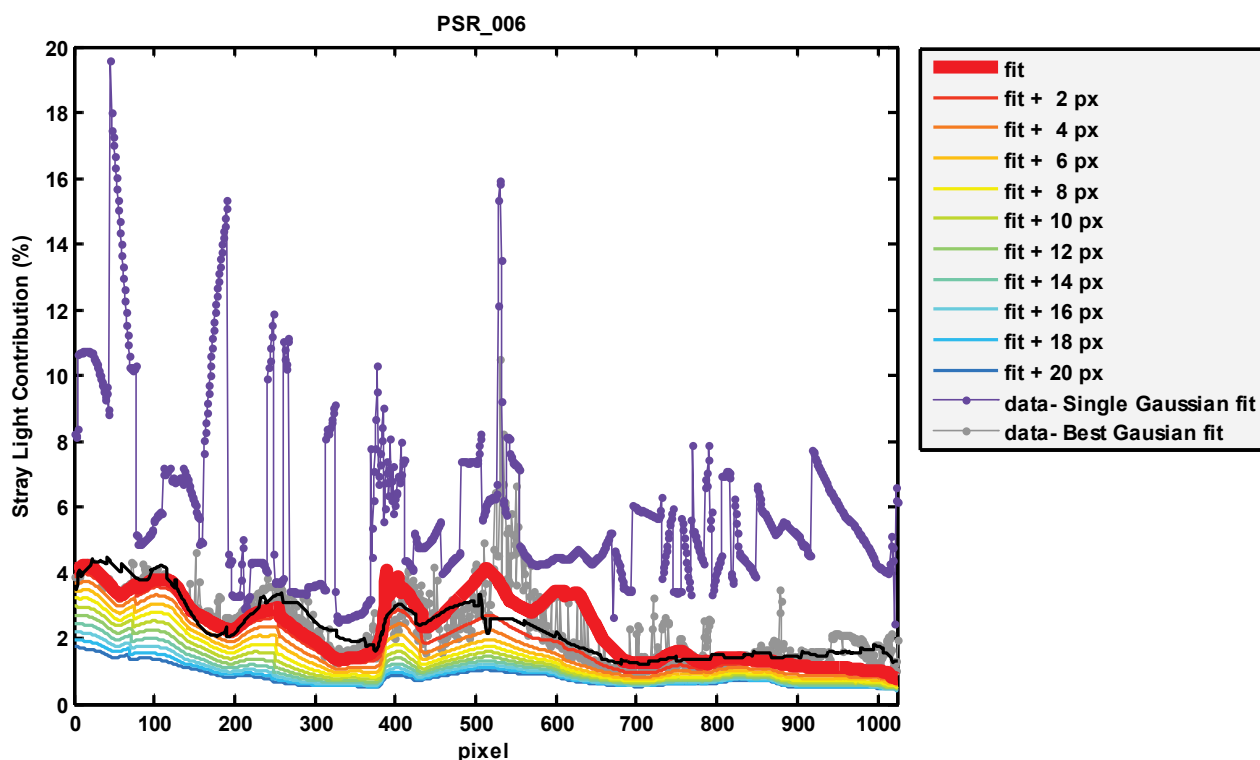


Figure 8: PSR_006 Percentage stray light contribution of a uniform spectrum. The black line represents the Stray Light Correction based on LSF measurements performed at PTB (Nevas *et al.*, 2014) for PSR_003.

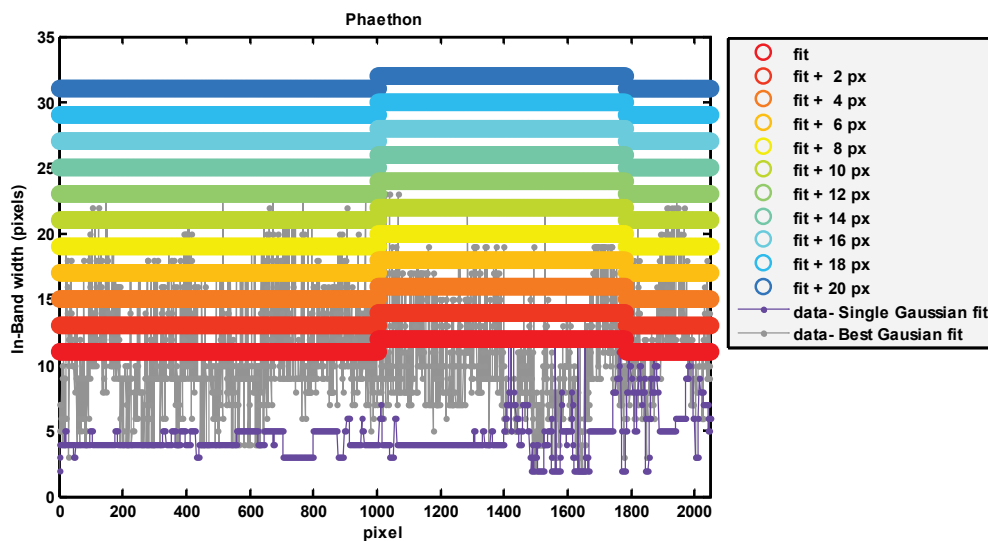


Figure 9: Selection of the In-Band region based on the agreement (better than 10%) between measurement and Gaussian fit. The violet line represents the single Gaussian fit , the gray line the best Gaussian fit and the red line the linear fit over the gray data.

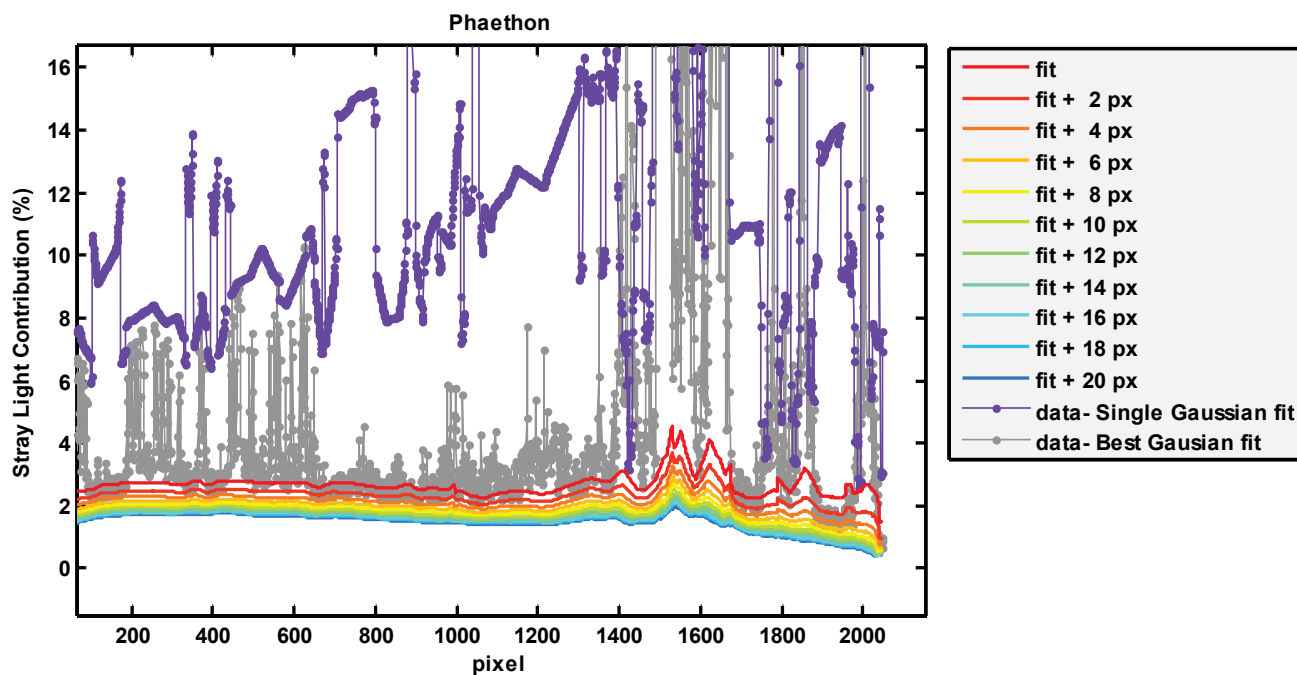


Figure 10: Phaethon: Percentage stray light contribution in of a uniform spectrum

6 Validation of Stray Light Correction

The validation of the stray light correction with respect to the background and IB width was done with PSR_006 measurements of an FEL lamp attenuated by different cut-off filters (460nm, 580nm, 800nm). In Figure 10 the test spectrum of the cut-off filter at 460 nm is shown. The cut-off filter blocks the irradiance at wavelengths less than 450 nm with an efficiency of better than 99.9%. It is expected that the test spectrum should be zero in that wavelength range. However we observe an offset of ~50 counts due to stray light contribution from longer wavelengths. The efficiency of the retrieved stray light corrections can be evaluated by analyzing this offset. The different choices of the IB width affect the percentage of stray light correction in the nearby pixels but not the background correction. The overall background correction is affected by the treatment of the LSF for negative values and noise. In Figure 9 an example of smoothed (light lines) and raw (darker lines) LSFs is shown, the impact is an average offset of -10 counts when the smoothed stray light correction matrix is applied to the test spectrum (Figure 10). Therefore the final stray light correction matrix for both instruments has been retrieved from the raw LSFs. Moreover we compare the stray light correction of PSR_006 measured with the ATLAS system with the one measured at PTB (Nevas *et al.* 2014) for a similar instrument PSR_003 (black line in figures 8 and 11). The similarities on the level and shape of the stray light contribution as well as the background correction show that the proposed in-band stray-light correction is able to correct for stray light well, validating the proposed method.

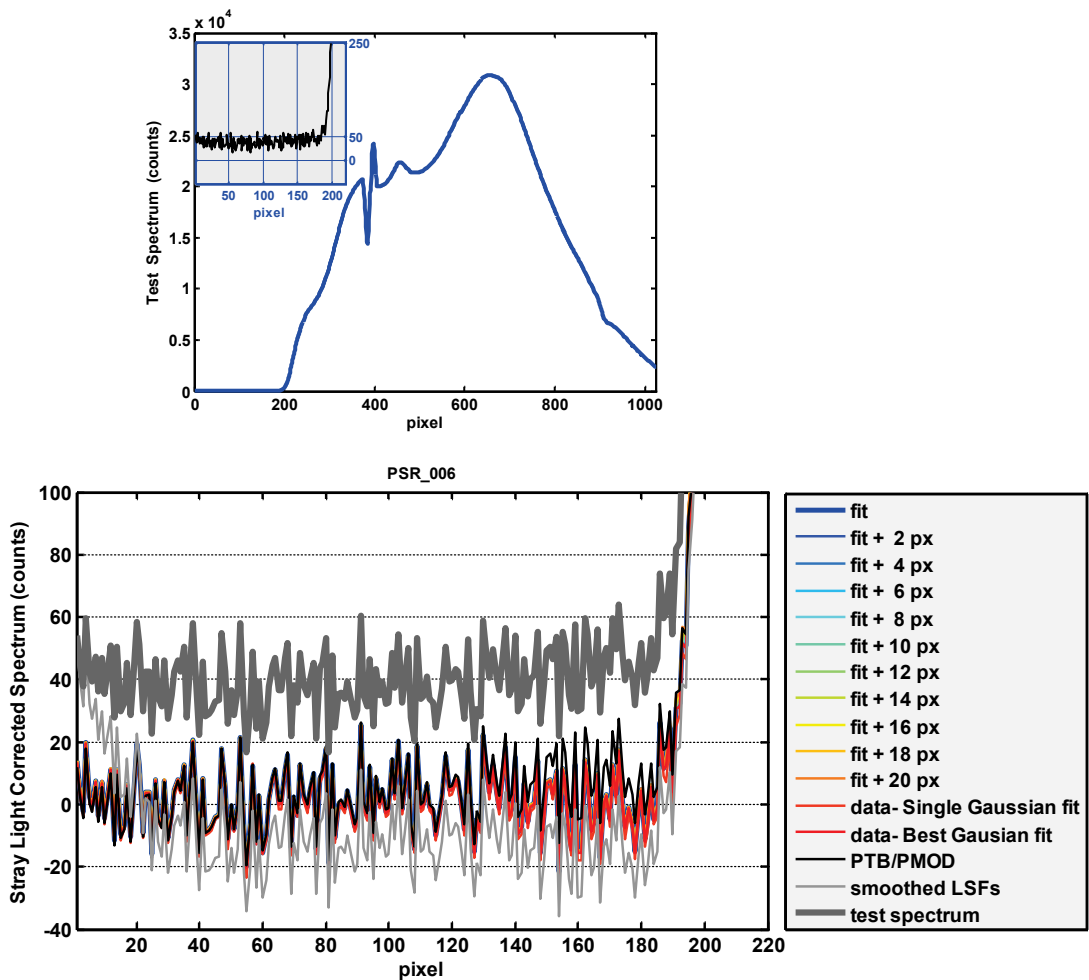


Figure 11: Dark corrected Signal of PSR_006 for a cut-off filter at 460 nm (up). Impact of various stray light correction matrices on the offset of the test spectrum (down).

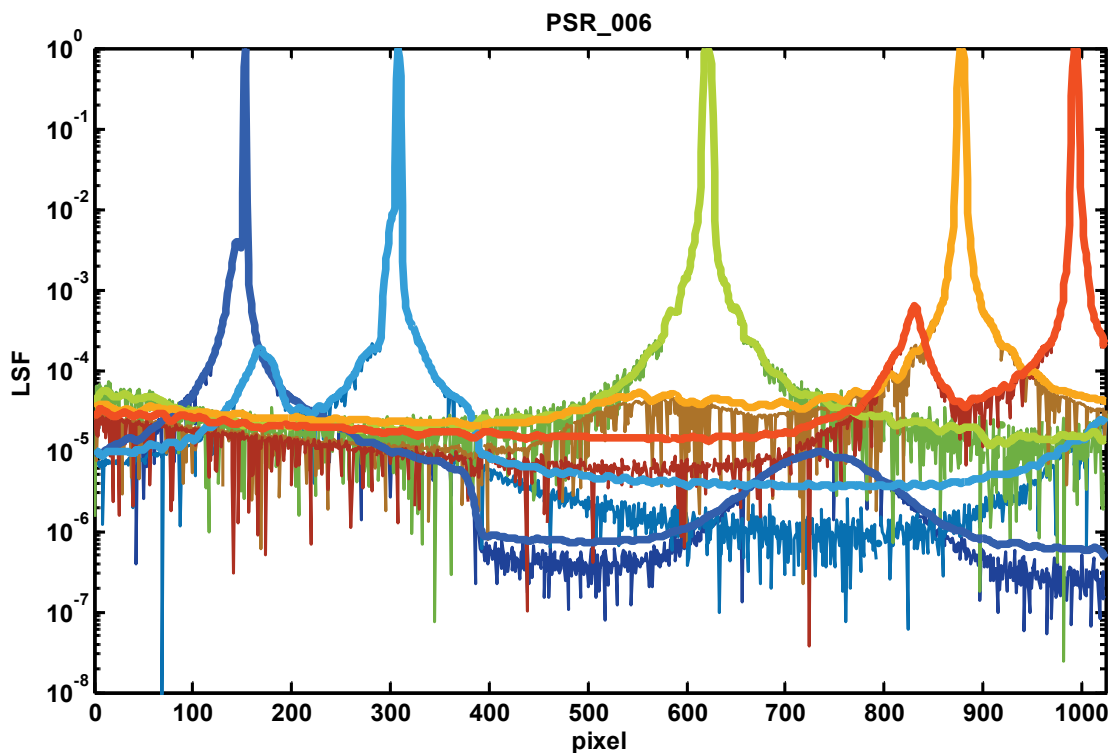


Figure 12: Example of smoothed (light lines) and raw (thick lines) LSFs of PSR_006.

7 Data archive

The measured data and products are archived in matlab format on the PMOD/WRC server, at ad.pmodwrc.ch/Institute/Projects/ATLAS/characterisations

8 References

Yuqin Zong, Steven W. Brown, B. Carol Johnson, Keith R. Lykke, and Yoshi Ohno, "Simple spectral stray light correction method for array spectroradiometers," *Appl. Opt.* **45**, 1111-1119 (2006)

S. Nevas, J. Gröbner, L. Egli, and M. Blumthaler, "Stray light correction of array spectroradiometers for solar UVmeasurements," *Appl. Opt.* **53**, 4313-4319 (2014).

The Dokumenten History

Version	Freigabedatum	Freigabe	Änderungen
1.0	17.8.2016	JG	NK, First Version of document